BLOOFINZ - Gulf of Mexico

Bluefin Larvae in Oligotrophic Ocean Foodwebs, investigations of nutrients to zooplankton: overview of the BLOOFINZ-Gulf of Mexico program

TRIKA GERARD[1], JOHN T. LAMKIN[1], THOMAS B. KELLY[2,3], ANGELA N. KNAPP [2], RAÚL LAIZ-CARRIÓN[4], ESTRELLA MALCA [1,5], KAREN E. SELPH [6], AKIHIRO SHIROZA[1,5], TAYLOR A. SHROPSHIRE [2,7], MICHAEL R. STUKEL [2], RASMUS SWALETHORP[8], NATALIA YINGLING [2] AND MICHAEL R. LANDRY [8,*]

[1]SOUTHEAST FISHERIES SCIENCE CENTER, NATIONAL MARINE FISHERIES SERVICE, NATIONAL OCEANIC AND ATMOSPHERIC ADMINISTRATION, MIAMI, FL 33149, USA, [2]EARTH, OCEAN AND ATMOSPHERIC SCIENCE, FLORIDA STATE UNIVERSITY, TALLAHASSEE, FL 32306, USA, [3]COLLEGE OF FISHERIES AND OCEAN SCIENCES, UNIVERSITY OF ALASKA FAIRBANKS, FAIRBANKS, AK 99775, USA, [4]INSTITUTO ESPAÑOL DE OCEANOGRAFÍA, CONSEJO SUPERIOR DE INVESTIACIONES CIENTIFICAS (IEO-CSIC), CENTRO OCEANOGRÁFIGO DE MÁLAGA, 29640 FUENGIROLA, SPAIN, [5]COOPERATIVE INSTITUTE FOR MARINE AND ATMOSPHERIC STUDIES, UNIVERSITY OF MIAMI, MIAMI, FL 33149, USA, [6]DEPARTMENT OF OCEANOGRAPHY, UNIVERSITY OF HAWAII AT MANOA, HONOLULU, HI 96822, USA, [7]DIVISION OF COASTAL SCIENCES, GULF COAST RESEARCH LABORATORY, UNIVERSITY OF SOUTHERN MISSISSIPPI, OCEAN SPRINGS, MS 39564, USA AND [8]SCRIPPS INSTITUTION OF OCEANOGRAPHY, UNIVERSITY OF CALIFORNIA, SAN DIEGO, 9500 GILMAN DR., LA JOLLA, CA 92039-0227, USA

*CORRESPONDING AUTHOR: mlandry@ucsd.edu

Corresponding editor: John Dolan

Western Atlantic bluefin tuna (ABT) undertake long-distance migrations from rich feeding grounds in the North Atlantic to spawn in oligotrophic waters of the Gulf of Mexico (GoM). Stock recruitment is strongly affected by interannual variability in the physical features associated with ABT larvae, but the nutrient sources and food-web structure of preferred habitat, the edges of anticyclonic loop eddies, are unknown. Here, we describe the goals, physical context, design and major findings of an end-to-end process study conducted during peak ABT spawning in May 2017 and 2018. Mesoscale features in the oceanic GoM were surveyed for larvae, and five multi-day Lagrangian experiments measured hydrography and nutrients; plankton biomass and composition from bacteria to zooplankton and fish larvae; phytoplankton nutrient uptake, productivity and taxon-specific growth rates; micro- and mesozooplankton grazing; particle export; and ABT larval feeding and growth rates. We provide a general introduction to the BLOOFINZ-GoM project (Bluefin tuna Larvae in Oligotrophic Ocean Foodwebs, Investigation of Nitrogen to Zooplankton)

and highlight the finding, based on backtracking of experimental waters to their positions weeks earlier, that lateral transport from the continental slope region may be more of a key determinant of available habitat utilized by larvae than eddy edges per se.

KEYWORDS: food web; productivity; lateral transport; feeding; larval growth; blue fin tuna; phytoplankton; zooplankton

INTRODUCTION

Understanding the ecology of pelagic ecosystems is a central goal of both fisheries oceanography and biological oceanography, although their approaches and emphases differ. From a fisheries perspective, feeding, growth and survival of larval fishes during their planktonic phase have long been considered key determinants of recruitment success and stock fluctuations (Hjort, 1914; Houde, 1987). Nevertheless, while larval fish studies generally consider the prey resources for larvae, they seldom extend to the complexities of lower food-web structure and function that determine how these resources arise. In contrast, studies from the biological oceanography perspective focus on details of lower-level processes—from nutrient sources and uptake to phytoplankton biomass and production to grazing interactions—but generally stop at the roles of zooplankton as consumers or mediators of organic matter export. While zooplankton provide the obvious link between these two perspectives, they are rarely connected in end-to-end system studies (Mitra et al., 2014), making it difficult to move beyond historical correlative relationships between fish larvae and their environments that may lose predictive power as systems are impacted by warming, stratification and altered phenology due to climate change (Rykaczewski and Dunne, 2010; Doney et al., 2012; Muhling et al., 2020). Progress toward mechanistic understanding that can be modeled and possibly used in future management tools will require the combined efforts and expertise of pelagic food-web ecologists and fisheries oceanographers working together to solve problems of mutual interest (Llopiz et al., 2014; Landry et al., 2019).

This issue contains papers from such a collaborative effort focusing on the larvae of Atlantic bluefin tuna (ABT, *Thunnus thynnus*) in the Gulf of Mexico (GoM) conducted on two cruises during the peak May spawning seasons in 2017 and 2018. Prior to this study, historical surveys of larval ABT in the GoM, beginning in the 1970s, had established a strong association between larvae and the outer edges of anticyclonic eddies that circulate in offshore oligotrophic waters of the Gulf (Muhling et al., 2010; Lindo-Atichati et al., 2012). A non-dimensional index of ABT larval habitat quality developed from these relationships had further been shown to account for the majority (58%) of interannual stock recruitment variability over a two-decade period (Domingues et al., 2016). However, despite this success in demonstrating the potential relevance of larval habitat variability to stock forecasting, the ecological characteristics of the larval habitat, beyond its general physical properties (temperature, salinity, depth), have not been investigated. Similarly, previous process-based ecological studies in GoM have mainly focused on the dynamics of the productive coastal margins, leaving the food-web relationships of the oceanic region largely unexplored. Our study sought to address knowledge gaps in both areas—ecological characteristics of ABT larval habitat and the general paucity of plankton food web and process studies in the oceanic GoM.

The BLOOFINZ-GoM project (Bluefin Larvae in Oligotrophic Ocean Foodwebs, Investigation of Nitrogen to Zooplankton) was designed to include traditional larval ABT surveys of abundance, feeding and growth rate measurements within the broader scope of system-level Lagrangian experiments focusing on nutrient sources, productivity and trophic interactions in eddy-edge habitats where larvae are generally found. While the oceanic GoM is highly oligotrophic, on average (Hidalgo-González et al., 2005; Hidalgo-González and Alvarez-Borrego, 2008), we hypothesized that eddy edges might have unique characteristics that enhance productivity, prey resources or food-web efficiencies in ways that benefit feeding and growth of larvae. Both nitrate and nitrogen fixation were considered viable sources of new N for productivity at eddy edges and evaluated for their respective contributions to ^{15}N isotope budgets and export rates. Additional component studies included the quantification of carbon biomass and community composition from bacteria to zooplankton, assessments of trophic pathways from production to micro- and mesozooplankton grazing, predation preferences and growth rates of ABT larvae, and several modeling syntheses of food-web flows, zooplankton biomass distributions, lateral transport and starvation-predation tradeoffs for larvae. In the sections below, we provide general overviews of ABT larval ecology, the GoM study site, sampling and experimental design,

characteristics and sources of the experimental water parcels and, finally, a summary of study components and their findings.

ABT IN THE GoM

ABT is one of the three large and broadly migrating bluefin species that exploit rich feeding grounds throughout temperate and subpolar regions of the major oceans (Pacific Ocean—*Thunnus orientalis*; Southern Ocean—*Thunnus maccoyii*). Unlike tropical tunas, which can reproduce over extensive areas throughout much of the year (Nishikawa *et al.*, 1985; Schaefer, 2001), bluefin species make long-distance migrations to spawn during relatively short periods in small geographical areas generally of the oligotrophic tropical/subtropical seas (Block *et al.*, 2001; Shimose and Farley, 2016; Muhling *et al.*, 2017). Growth and survival during the first few weeks of life thus depend critically on the conditions that larvae experience within these specific habitats and times of year. Due to their shallow vertical distributions (0–25 m) in the mixed layer (Davis *et al.*, 1990; Habtes *et al.*, 2014), bluefin tuna larvae are also directly exposed to the impacts of projected climate change—warmer surface temperature, stratification-diminished productivity and increased acidity (Bopp *et al.*, 2001; Behrenfeld *et al.*, 2006; Doney *et al.*, 2012; Chust *et al.*, 2014; Fu *et al.*, 2016), whereas juveniles and adults can more easily mitigate such impacts by active thermoregulation, deeper distributions or relocation to more suitable habitats with shifting ocean province boundaries. Larvae thus represent an especially vulnerable life history period that can impact interannual recruitment variability and long-term trends of the bluefin species.

The International Commission for the Conservation of Atlantic Tunas (ICCAT) divides ABT into two management units, eastern and western stocks, conventionally separated by the 45°W meridian. While the stocks mix in North Atlantic feeding grounds, they spawn separately (Carlsson *et al.*, 2007; Boustany *et al.*, 2008). The western stock spawns almost exclusively in the GoM (Richards, 1977; Scott *et al.*, 1993), although some larvae have also been found along the Yucatan Peninsula (Muhling *et al.*, 2011), the Bahamas (Lutcavage *et al.*, 1999; Goldstein *et al.*, 2007; Rooker *et al.*, 2007) and the western Slope Sea (Richardson *et al.*, 2016). The eastern stock, currently about an order of magnitude more abundant than the western stock, spawns in the Mediterranean Sea (García *et al.*, 2004; Alemany *et al.*, 2010). However, strong connectivity between ABT stocks is indicated by genetic evidence (Carlsson *et al.*, 2004, 2007; Boustany *et al.*, 2008; Puncher *et al.*, 2018; Johnstone *et al.*, 2021) as well as from

otolith microchemistry (Rooker *et al.*, 2003, 2008), otolith isotopes (Rodríguez-Ezpeleta *et al.*, 2019), electronic tagging (Block *et al.*, 2005) and parasite studies (Rodríguez–Marín *et al.*, 2008).

Plankton surveys targeting larval ABT have been undertaken annually in the northern GoM by the NOAA National Marine Fisheries Service since 1977 following a coarse fixed-grid station plan, producing distributional relationships that link habitat structure in the GoM to recruitment variability of the western ABT stock. Adult ABT spawn in waters within well-defined ranges of sea surface temperature (SST = 24–28°C) and salinity (35.5–37.0 psu) (Muhling *et al.*, 2010, 2011). ABT larvae are also quantitatively more abundant in the outer boundaries of anticyclonic mesoscale eddies and hydrographic fronts in both the GoM (Lindo-Atichati *et al.*, 2012) and the Mediterranean Sea (Garcia *et al.*, 2005; Alemany *et al.*, 2010). Building upon these relationships, Domingues *et al.* (2016) developed a dimensionless index of larval presence/absence using larval survey data and satellite measurements of SST and sea surface height (SSH) that successfully captured the general features of larval spatial distributions and temporal variability in the GoM. Interannual mean differences determined from that physical habitat index explained 58% of western ABT stock recruitment variability over the two-decade period from 1993 to 2011, demonstrating the relevance of larval habitat quality in the GoM to ABT fisheries management. Despite the strong correlation, however, no mechanisms were advanced to connect larval feeding, growth or survival to specific ecological or biogeochemical properties of the favorable habitats.

Larval cooperative studies in the GoM have provided insights into multiple aspects of tuna larval ecology and biology, particularly growth and food web dynamics (Laiz-Carrión *et al.*, 2015, 2019; Malca *et al.*, 2017). Similarly, while prior studies of feeding and growth of larval ABT in the GoM have contributed substantial new knowledge to understanding mean rates and variability during early life history, they have largely been done outside of the broader context of system-level production and trophic investigations. For example, growth relationships for larvae based on analysis of daily otolith rings have shown large individual variability, with 8-day-old larvae ranging in length from 4 to 9 mm and 5 mm larvae varying in age from 5 to 10 days (Scott *et al.*, 1993), that has not been explained by adequate sampling of feeding rates or prey availability. Malca *et al.* (2017) also found significant differences in growth strategies of ABT larvae in the GoM and Mediterranean Sea (Balearic Islands), with the former growing faster in length (long and skinny) and the latter adding more biomass, but the influences of food or feeding differences

were unclear. In GoM larval feeding studies, Llopiz et al. (2015) and Tilley et al. (2016) both reported variable diets during larval development, with young larvae feeding on copepod nauplii and gradually transitioning to larger prey categories as the larvae developed. Larval feeding success, defined as the percentage of larvae with at least one ingested prey, was observed to increase rapidly with size, from ~17% for 3 mm larvae to 50–70% for 4–5 mm larvae to ~100% for >6-mm larvae (Tilley et al., 2016). Llopiz et al. (2015) provided the first evidence of significant ABT larval feeding on appendicularians and the early onset of piscivory. The 2010 data from Tilley et al. (2016) are also confounded by large numbers of barnacle larvae consumed in the downstream flow from the Deepwater Horizon oil spill, suggesting opportunistic feeding on an unusual mass spawning event of barnacles from numerous oil derricks in the region that may have been precipitated by the spill or cleanup chemicals. Additionally, neither Llopiz et al. (2015) nor Tilley et al. (2016) reported ambient abundances of zooplankton prey from field sampling; thus, it is not known whether the consumed prey in their studies were strongly selected for, reflecting larval feeding preference, or eaten based on availability. These are all areas where concurrent studies of pelagic ecosystem ecology and larval ABT feeding and growth would help to advance understanding of habitat quality effects on larval success in the GoM.

THE STUDY AREA

The GoM is a small marginal sea surrounded almost entirely by the southern USA, eastern Mexico and the island of Cuba; almost half of its 1.6×10^6 km² surface area is continental shelf (Fig. 1). Large inputs of freshwater and nutrients from 22 rivers, most notably the Mississippi-Atchafalaya complex in the northern Gulf, contribute to high productivity and pronounced biological variability on and along the Gulf shelf (Fahnenstiel et al., 1995; Lohrenz et al., 1999, 2008; Rabalais et al., 2002; Liu and Dagg, 2003; Qian et al., 2003; Wawrik and Paul, 2004) that contrast sharply with the general oligotrophy of the oceanic GoM (Hidalgo-González et al., 2005). Despite high productivity, however, physical conditions of the shelf regions are typically outside of the narrow environmental envelopes associated with the presence of ABT larvae (Muhling et al., 2010). This likely reflects the distributional preferences, physiological constraints or sensory capabilities of adult ABT that aggregate along deeper slope waters prior to spawning (Teo et al., 2007), but it is also seen as a significant survival advantage for larvae to avoid the high-risk predatory environment of the
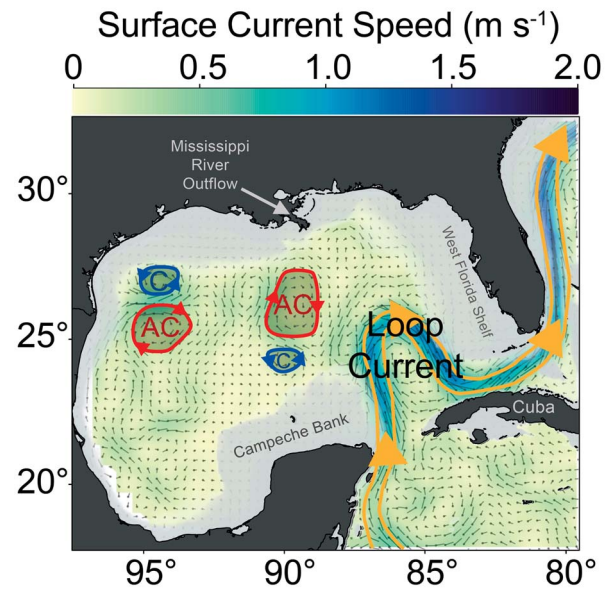

Fig. 1. Schematic representation of the GoM study region illustrating flow of the LC, warm-core anticyclonic (AC, red) loop eddies, cool-core cyclonic (C, blue) eddies and major constraints of regional geography. Continental shelf margin (<200-m depth) is light shaded. Flow field details are from satellite image of 12 May 2017.

more productive waters (Bakun and Broad, 2003; Bakun, 2006).

The Loop Current (LC) is a major driver of circulation in the oceanic GoM, both directly and indirectly through its role in generating eddies (Fig. 1). The rapidly moving current enters the GoM along the Yucatan Peninsula, turns eastward and southward (the "loop") in the NE Gulf and exits as the Florida Current via the Florida Straight (Leipper, 1970; Elliott, 1982; Vukovich, 2007). When the LC extends northward into the GoM, large anticyclonic loop eddies break off periodically to become major westward-propagating features of mesoscale circulation with lifespans of many months to a year (Maul and Vukovich, 1993; Bracco et al., 2016). LC interactions with bathymetry of the Yucatan Peninsula also shed cyclonic eddies that contribute to mesoscale variability in the offshore waters (Chérubin et al., 2006).

The LC core flow and the very warm water that it transports into the GoM from the Caribbean Sea are not ideal larval ABT habitat (Muhling et al., 2010) and appear to be avoided by ABT adults, which dive deeply (>500 m) under that area during entry and exit from the Gulf (Teo et al., 2007). Within the remaining GoM domain that constitutes larval habitat (i.e. not LC or shelf), several mechanisms associated with eddy edges or circulation effects might benefit larvae, including direct nutrient stimulation of productivity (Biggs, 1992;

Biggs and Ressler, 2001; Brannigan, 2016), convergent flows that enhance densities and encounter rates of larvae with zooplankton prey (Bakun, 2006, 2013) and physical transport of shelf productivity into the central Gulf region (Biggs and Müller-Karger, 1994; Merino, 1997; Melo Gonzalez *et al.*, 2000). Model simulations have demonstrated that submesoscale symmetric instabilities in anticyclonic eddies can draw nutrients up from the thermocline and distribute the nutrients in rings around the eddy core (Brannigan, 2016). Flow interactions of eddy pairs have been observed to transport filaments of shelf productivity 100–200 km into the central Gulf waters (Biggs and Müller-Karger, 1994), and even small intrusions of the Mississippi River plume offshore (3% of surface area) can account for a large fraction (43%) of the oceanic region's production (Wawrik and Paul, 2004). However, how such hypothetical enhancement effects are actually manifested in the lower level food web dynamics of ABT larval habitat are unstudied and unknown.

While significant environmental heterogeneity along the GoM margins and eddy features are well recognized (Zimmerman and Biggs, 1999; Biggs and Ressler, 2001), previous research has characterized the oceanic GoM as a stratified oligotrophic system with low biomass, low productivity and distinct communities, on average, compared with the shelf region (Wawrik and Paul, 2004; Hidalgo-González *et al.*, 2005; Hidalgo-González and Alvarez-Borrego, 2008; Chakraborty and Lohrenz, 2015). It is nonetheless a very sparsely studied region, especially with respect to trophic processes. The literature reveals no prior estimates of mesozooplankton carbon biomass and community grazing in the deep GoM, and only two experiments have measured microzooplankton grazing rates in waters with oceanic surface salinity ≥35 psu (Strom and Strom, 1996). Similarly, most estimates of phytoplankton production in the oceanic GoM come from models and satellite data rather than direct field measurements (Hidalgo-González *et al.*, 2005; Hidalgo-González and Alvarez-Borrego, 2008; Müller-Karger *et al.*, 2015; Gomez *et al.*, 2018). Hidalgo--González *et al.* (2005), for example, used a general non-spectral photosynthetic model with SeaWIFS monthly averaged Chl*a* and light extinction values to determine a ~2-fold seasonal cycle in primary production in the oceanic GoM, averaging 370–440 mg C m^{-2} d^{-1} during "cool" winter–spring months and 220–240 mg C m^{-2} d^{-1} during "warm" summer–fall months. The May–June ABT spawning season occurs critically at the end of the cool period where details of the productivity transition and spatial variability are potentially important. Model estimates of new production (NP) in the oceanic GoM, based on mean nitrate profiles and parameterizations

from other regions (13–26 mg C m^{-2} d^{-1}; Hidalgo–González *et al.*, 2005), are two orders-of-magnitude lower than rates on the Mississippi River-influenced shelf and also 2–5 times lower than measured rates of carbon export in GoM eddies (Hung *et al.*, 2004, 2010), suggesting poorly known relationships or missing terms.

Beyond potential relevance to ABT larvae, the N sources and magnitude of NP are first-order questions for understanding lower food-web structure, productivity and trophic interactions in the oceanic GoM. A substantial role of nitrogen fixation is suggested in the oceanic GoM by significantly lower average δ^{15}N values for oceanic (2.8 ± 1.4‰) versus neritic zooplankton (5.5 ± 1.1‰) (Dorado *et al.*, 2012). Modest rates of N$_2$ fixation have been measured on the GoM coastal margins (Mulholland *et al.*, 2006, 2014; Holl *et al.*, 2007) but could be greatly enhanced in convergent eddy fronts where large buoyancy-regulating and diazotrophy-associated phytoplankton, such as *Trichodesmium* and *Rhizosolenia*, are known to concentrate (Yoder *et al.*, 1994; Olson *et al.*, 2015). Eddy boundaries, however, are also complicated areas where vertical mixing processes, nitrogen fixation and horizonal advection may all contribute importantly as N sources (Mulholland *et al.*, 2006).

SAMPLING AND EXPERIMENTAL PROGRAM

The BLOOFINZ-GoM cruise plan combined two main activities. The first was to survey areas to locate patches of ABT larvae to study. The second was to conduct Lagrangian experiments, termed *cycles*, during which chosen water parcels were marked by satellite-tracked drifters and sampled repeatedly over 2–4 days to assess biogeochemical and community characteristics, productivity and trophic interactions.

ABT larvae were surveyed according to established protocols, using standardized 10-min oblique tows (~2.2 kts) in the upper 25 m with a 90-cm diameter bongo frame with two 505-μm Nitex mesh nets (Habtes *et al.*, 2014; Laiz-Carrión *et al.*, 2015). These were generally followed by a 300-m CTD cast, while the net collection was processed. The content of one of the bongo nets was immediately preserved in 95% ethanol for later sorting. The other net was rinsed with seawater, concentrated with a 333-μm sieve, cooled on ice and examined live by experienced ichthyoplankton taxonomists. Larval ABT were identified by their dorsal melanophore pattern that distinguishes ABT from other *Thunnus* species or similarly shaped scombrids (Richards, 2005). Larvae-positive areas were defined by finding at least five ABT larvae in the one net examined on two consecutive tows.

Larval surveys were guided by Bluefin Index habitat maps refreshed daily from the satellite measurements of SSH, temperature and currents following the criteria of Domingues *et al.* (2016). Figures 2 and 3 show sampling locations for cruises NF1704 and NF1802, respectively, along with habitat maps illustrating system features at times when cycle experiments were conducted. Details of sampling locations, larval abundances and mean temperature, salinity and chlorophyll *a* fluorescence from CTD casts are given in Supplementary Table S1 (see online supplementary data for a color version of this table). NF1704 departed Key West, Florida, on 5 May 2017. After crossing the LC, abundant ABT larvae were encountered in the first area sampled, the NW edge of a weak anticyclonic loop eddy on the western side of the LC with an above-average, but not high, habitat index (Fig. 2A and B). Experimental Cycle 1 (C1) was initiated in this larvae-positive patch and ran from 10 to 14 May, with larval abundances averaging ∼29 per tow through the first two days. Larval abundances decreased subsequently, and we believe that the drifter had slipped out of the patch by the end of the cycle (Supplementary Table S1, see online supplementary data for a color version of this table). We next surveyed both the western and eastern edges of the AC eddy with high index scores in the vicinity of 26°N, 90°W (Fig. 2C). While only one larva was found in both areas, a short 2-day cycle experiment (C2, 16–18 May) was conducted on the southeastern of this high-quality habitat without larvae, as a contrast to C1. Following a mid-cruise port stop in Progresso, Mexico (Yucatan), additional survey transects were made across the eastern and northern edges of the prominent AC eddy with high habitat scores in the western GoM (vicinity of 26°N, 94°W) and then across the northwestern edge of the same eddy investigated previously for C2 (Fig. 2D). None of these latter survey sites were larvae positive, but, with limited cruise time remaining, the C3 experiment was conducted (26–30 May) in the latter area. On return transit, three stations sampled at ∼26.3°N, 88.67°W, slightly to the west of the original location of the C1 experiment, showed that the area still had relatively high larval abundances (17.5–24.5 larvae per tow; Supplementary Table S1, see online supplementary data for a color version of this table).

Cruise activities for NF1802 were limited to US waters and shortened by a long transit (27 April departure from Jacksonville, FL) at the start of the cruise and a premature ending for repairs. Nonetheless, all features in the study area with high index scores were surveyed at least briefly. The high index area off the southern Florida shelf was sampled from 30 April to 1 May (Fig. 3A and B). Two areas of high index north of the EEZ border (26–27°N,

88°W) and the eastern side of the major AC eddy feature (∼27°N, 88–89°W) were sampled on 1–2 May. The northern edge of the AC eddy adjacent to the northern Gulf slope was sampled in three transects on 3–4 May (Fig. 3A and B). Larvae were found in stations sampled on two crossings of the northwestern edge of the eddy (27.5°N, 89.7°W; Fig. 3A), but we missed the opportunity to conduct an experiment in this vicinity. C4 experiments were subsequently initiated without larvae on the northeastern edge of the same feature and followed a rapidly moving southward flow that connected two eddies with high index scores (5–9 May; Fig. 3A and B). After a port stop in Pensacola, Florida, sampling of a newly revealed area of above-average habitat index in the northeastern Gulf (14 May; Fig. 3A and C) yielded the highest recorded ABT larval catches for GoM ichthyoplankton surveys in over a decade. C5 experiments were conducted in these larvae-positive waters with slow westward flow from 15 to 19 May and additional larval-positive stations were sampled before ending the cruise in Pascagoula, MS, on 20 May.

Each of the five cycles conducted involved a coordinated series of sampling and experimental activities to measure hydrography, nutrient concentrations, biomass and composition of the plankton community, and process rates (phytoplankton nutrient uptake, productivity and growth; micro- and mesozooplankton grazing; export; and ABT larval feeding and growth rates when present). A sediment trap array with a mixed-layer (15 m) drogue was deployed the full duration of each cycle to measure export fluxes at three depths (Stukel *et al.*, 2015, 2016). A second array was also deployed to mark the patch and to serve as a platform for daily 24-h bottle incubation experiments under *in situ* temperature and light conditions in net bags attached to a wire hanging below the surface float (Landry *et al.*, 2009). Daily pre-dawn CTD casts collected water from 6 depths over the euphotic zone (EZ) for measuring daily profiles of nutrients and microbial community biomass and composition (Chl*a*, HPLC pigments, particulate C and N, flow cytometry and microscopy) and filling bottles for experimental measurements of primary production (^{13}C-bicarbonate), nitrate-based NP (^{15}N nitrate) and rates of phytoplankton growth and microzooplankton grazing (dilution experiments). Additional CTD casts were done for shipboard experiments of ammonium and nitrate uptake and primary production, for large-volume samples for *Trichodesmium* abundance and for ^{238}U-^{234}Th disequilibrium estimates of export fluxes. Net tow samples (200-μm mesh) were collected daily at midday and midnight for biomass and grazing assessments (gut fluorescence) of size-fractioned mesozooplankton. Bongonet sampling for ABT larvae continued throughout the cycles at ∼3–4 h intervals, with daylight noon samplings
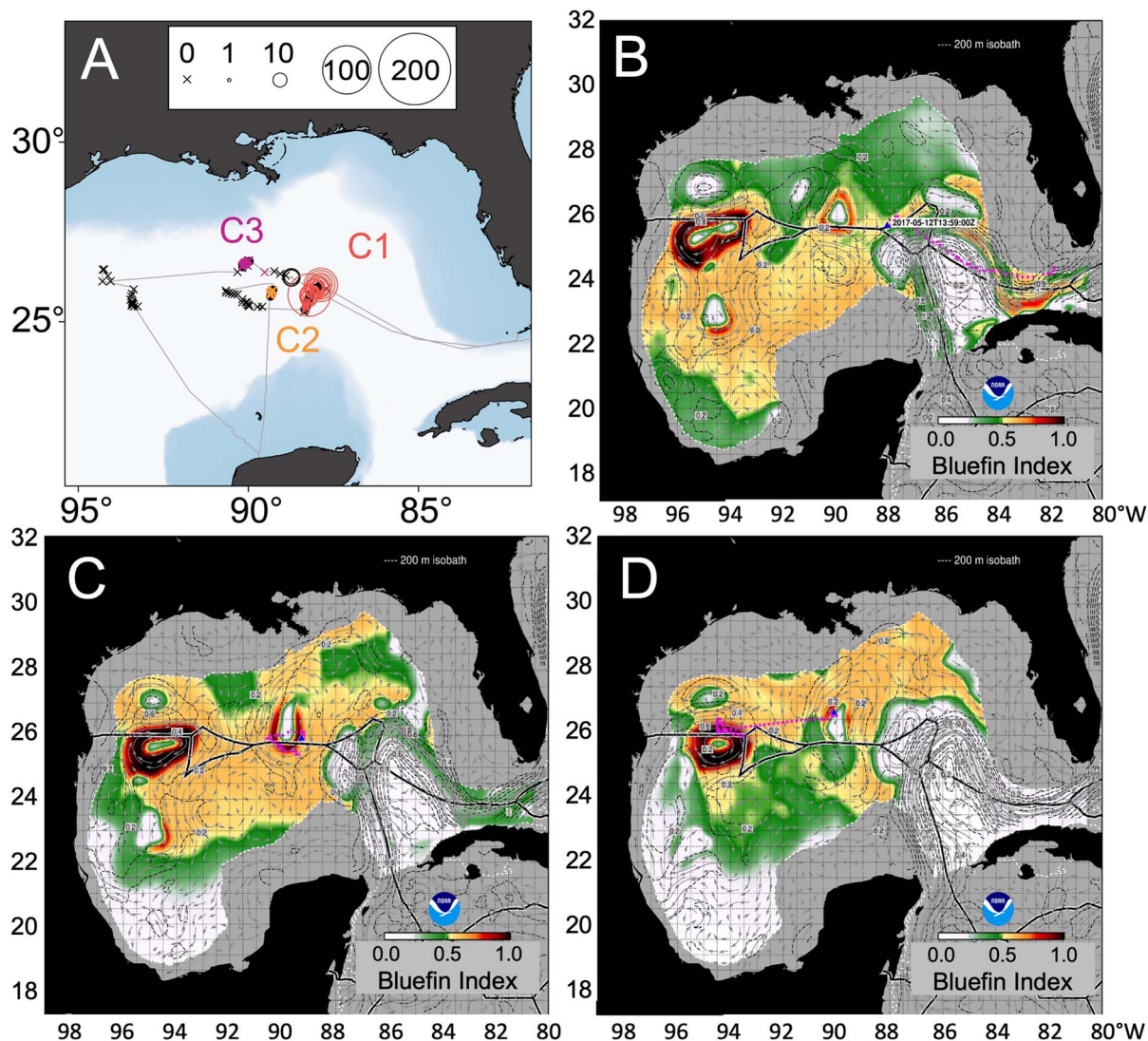
Fig. 2. Sampling locations and ABT larval habitat maps that guided survey sampling for cruise NF1704 in May 2017. (A) Sampling locations with bubble plots showing ABT larvae catches in standard survey bongo tows (one net or mean of both sides). Cycles 1–3 (C1–C3) are denoted by red, orange and purple symbols, respectively. Fine lines mark the cruise path. (B) Habitat map for 12 May during C1 experiment. (C) Habitat map for 17 May representing conditions during the C2 experiment. (D) Habitat map for 27 May during sampling of the western AC loop eddy and the start of C3. Boundaries of national and international waters are shown as the irregular lines that bisect the habitat maps.

generally paired with tows with a fine (53 μm) mesh net to collect the size range of available prey for larvae in the upper 25 m.

CHARACTERISTICS AND SOURCE WATERS OF ABT LARVAL HABITAT

Although ABT larvae were found in abundance at only two of the experimental cycles, C1 and C5, overall sampling of all sites for both cruises shows narrow

ranges of temperature (24–27°C) and salinity (35.5–36.5 psu) variability in the upper 25 m, whether larvae were present or not (Fig. 4). C1 environmental conditions were on the cooler and more saline sides of these ranges compared with C5, but these differences are unlikely to be meaningful to habitat quality for larvae. Our survey sampling results were notable in finding very few to no larvae at the edges of mesoscale eddies with the highest predicted Bluefin Index habitat quality scores based on prior research (the red-to-brown colored rings in Figs 2A–C and 3B). This prompted consideration of
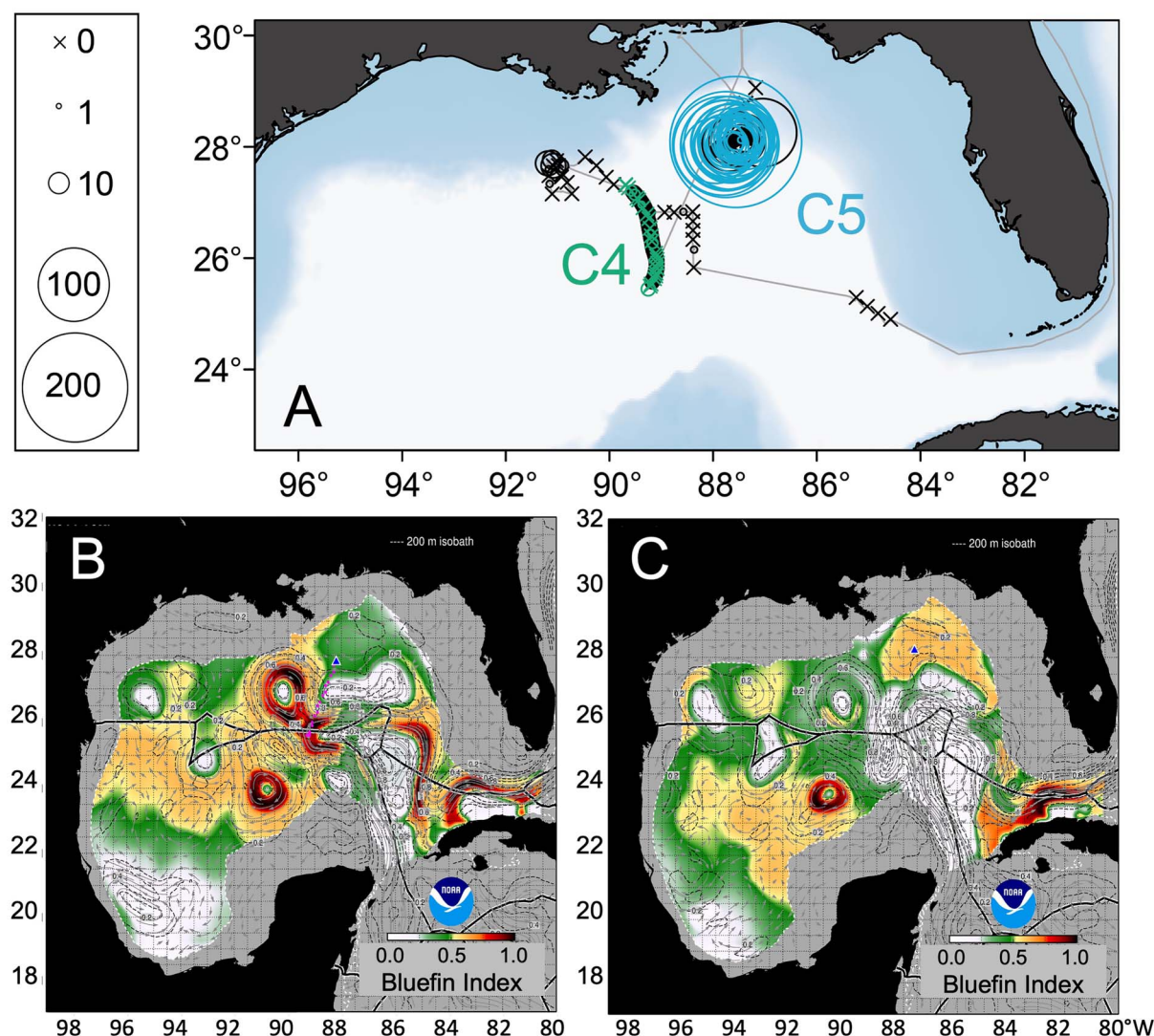
Fig. 3. Sampling locations and ABT larval habitat maps that guided survey sampling for cruise NF1802 in April–May 2018. (A) Sampling locations with bubble plots showing ABT larvae catches in standard survey bongo tows (one net or mean of both sides). Cycles 4–5 (C4–C5) are denoted by green and blue symbols, respectively. Fine lines mark the cruise path. (B) Habitat map for 8 May during early sampling off the south Florida slope and the central AC loop eddies leading to the C4 experiment. (C) Habitat map for 17 May representing conditions during the C5 experiment in the northeastern GoM. Boundaries of national and international waters are shown as the irregular lines that bisect the habitat maps.

other factors, particularly the source of waters of larval patches, that might be more important determinants of larval presence or absence in the different sites examined than the specific physical properties in the Domingues et al. (2016) index. One contributing factor could be depletion of the spawning stock of large ABT adults in the GoM to the point where only a small fraction of the favorable habit can be occupied, with spawning locations contracted to narrow favorable areas.

To investigate the source locations for water parcels sampled in cycle experiments, we conducted a backtracking modeling analysis in which we released 500 virtual floats (i.e. 2D Lagrangian particles) at the locations and times of the recorded drifter positions from each of the cycle experiments. To isolate dispersion related to observed non-Lagrangian motions (i.e. "slippage") of the drift array, floats were launched uniformly along the drift path during the first 24 h of each cycle. Surface velocity fields were provided by the reanalysis data product OSCAR (ESR, 2009), and the floats were tracked backward in time using a 4th-order Runge–Kutta algorithm with a 1-h time step and a model duration of ∼8 weeks total (April–June), or 6 weeks for each individual experiment. Subgrid scale dispersion was parameterized
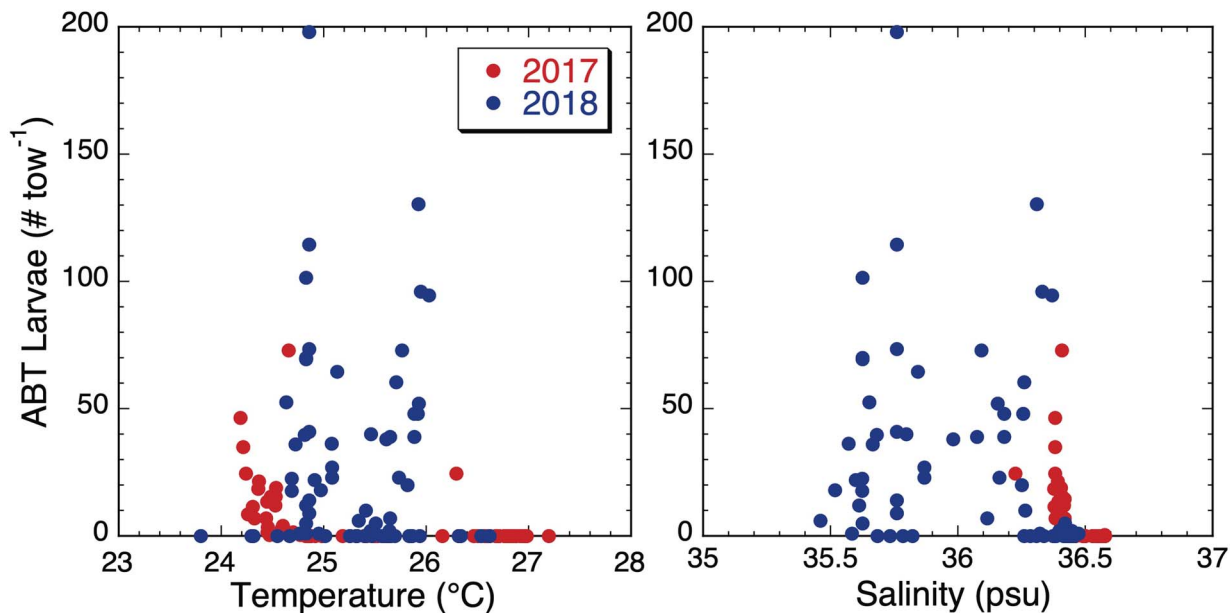
Fig. 4. Mean temperature and salinity characteristics of GoM waters where ABT larvae were collected on 2017 and 2018 cruises. Larval abundances are for standard 10-min oblique tows in the upper 25 m with a 90-cm bongo net frame with 505-μm mesh nets (one net side or mean of both sides). Temperature and salinity are mean values for the 0–25 m depth stratum from CTD casts taken immediately after the net tows or interpolated from adjacent casts for the two locations.

with a random-walk perturbation corresponding to a horizontal eddy diffusivity of 20 m^2 s^{-1}, a value consistent with previous regional biogeochemical models (Shropshire *et al.*, 2020). This approach assumes that the floats stay within the surface mixed layer, which may not be representative of actual particle behaviors in convergence or divergence zones. Nonetheless, the approach does quantify lateral length scales and the general degree of connectivity within the basin flows yielding a reasonably well-resolved picture for how water parcels would have been transported in the GoM prior to our experiments.

C1 and C5 demonstrate strong coastal connectivity with >50% of floats tracking back to the near-coastal slope-margin domain along the northeastern GoM (Fig. 5). Circulation patterns for C5 show that nearly all particles clustered ∼50 km southwest of the Florida panhandle 2–4 weeks prior to our initial sampling (Fig. 5F), indicating an especially strong coastal coupling for this cycle with very high larval abundances. C1 also shows strong connectivity to this area 2–4 weeks prior to our sampling of these waters far out in the central GoM (Fig. 5B). Despite their different locations, the shared feature of these two cycles with abundant ABT larvae is that they trace back to the same general area over the approximate duration of a larvae's planktonic existence,

which we interpret as pointing to a hot spot of spawning activity along the northeastern slope.

In comparison, back-trajectories for water parcels of the C2 and C3 experiments, which contained little to no larvae, were retained within the central GoM region for the extent of their prior histories of 2–6 weeks (Fig. 5C and D). Experiment C4 shows large-scale connectivity and dispersion patterns throughout the central GoM, with floats covering ∼1000 km over the modeled timeframe (horizontal currents of 0.5–1 m s^{-1}) (Fig. 5E). Some C4 water parcels come from as far as the Campeche Bank to the south, but most cycle rapidly off the northern slope south of Louisiana. While we observed some larvae close to the shelf break on northwestern slope in this flow regime (Fig. 3A), our choice of C4 starting site appears to have missed connecting to these source waters during at least the previous two weeks.

We conclude from this retrospective back-trajectory analysis that the physical (or ecological) characteristics of the anticyclonic loop eddy edges may be less important in defining ABT larval habit quality per se compared with their roles as physical transport mechanisms entraining or moving source water from major spawning locations. As will be further noted below, several other findings from the experimental and modeling results also point to the importance of lateral transport from the near-shelf
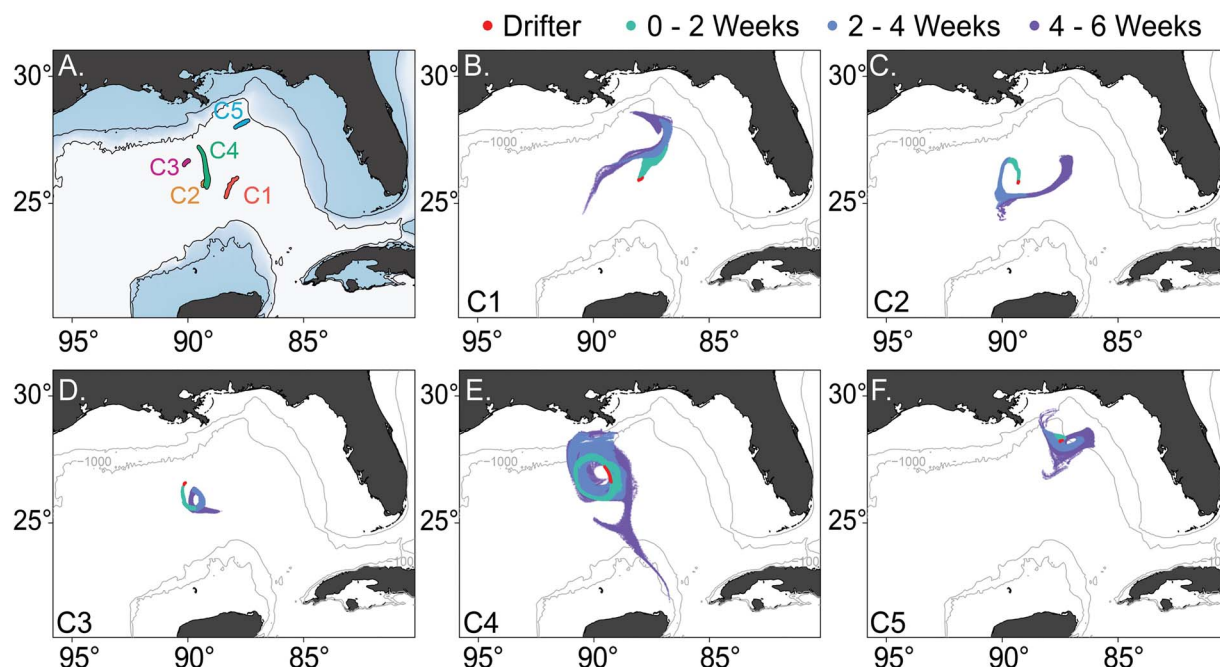
Fig. 5. Retrospective analyses of source water flows based on back-trajectories of virtual surface floats released along the drift path of C1–C5 experiments. (A) Locations and drift trajectories of C1–C5. (B–F) Backward projections of surface source waters to C1–C5, respectively, for 2–6 weeks prior to initial sampling based on surface velocity fields of the OSCAR reanalysis data product.

environment as a significant factor in resolving predation and export balances.

OVERVIEW OF MAJOR STUDY RESULTS

For this section, we divide results of the BLOOFINZ-GoM cruises into three broad themes: (i) plankton dynamics and flux relationships; (ii) the oceanic GoM as a larval habitat for ABT and (iii) comparisons of the GoM to other open-ocean systems. Under each theme, we first give a brief overview of the components of the project that relate to the theme, then present a bullet-point summary of key findings that can be found in the noted component publications.

Plankton dynamics and flux relationships

The BLOOFINZ cruises differ from previous GoM studies in taking a system-level, process-oriented approach involving complementary measurements of phytoplankton and zooplankton community biomass, composition and process rates over the EZ at several locations. These data provide the first depth-integrated assessments of phytoplankton group contributions to carbon standing stocks, productivity and grazing in the region, as well

as site-integrated assessments of primary production, NP and export. Selph *et al.* (2022) provide details of the phytoplankton community biomass, size structure, composition, depth distribution and spatial variability based on complementary analyses by microscopy, flow cytometry and HPLC pigments. Yingling *et al.* (2022) present estimates of net primary production (NPP) and NP based on uptake rates of $H^{13}CO_3^-$, $^{15}NO_3^-$ and $^{15}NH_4^+$ and use a Bayesian Markov Chain Monte Carlo approach to parameterize nutrient and light effects on growth rates of five phytoplankton taxa. Landry *et al.* (2022) report community and group-specific rate estimates for phytoplankton growth and microzooplankton grazing based on depth profiles of dilution experiments. Landry and Swalethorp (2022) provide size-fractioned biomass, isotopes and grazing rates for mesozooplankton and assess trophic structure and growth-grazing balances for the phytoplankton community. Stukel *et al.* (2022a) evaluate the efficiency of the GoM biological carbon pump based on export measurements from ^{234}Th-^{238}U disequilibrium and sediment trap collections at three depths. Knapp *et al.* (2022) apply a $\delta^{15}N$ budgeting approach to evaluate the relative importance of subsurface NO_3^- and N_2 fixation for supporting net food web process and export in the oceanic GoM. In additional synthetic studies presented elsewhere, Shropshire *et al.* (2020) configure a

physical-biogeochemical model (NEMURO-GoM) that is validated against mesozooplankton biomass and grazing rates and other constraints from the BLOOFINZ cruises, and Kelly *et al.* (2021) evaluate the contribution of laterally sourced organic matter to export using the NEMURO-GoM model and satellite remote sensing products. Significant findings from the dynamics and flux portion of the study include the following:

- Euphotic-zone integrated values of Chl*a* averaged 10.3–10.4 mg m^{-2} on the two cruises, and autotrophic carbon ranged from 460 to 1 270 mg m^{-2}, with ∼2-fold higher carbon in the DCM compared with ML values (Selph *et al.*, 2022). Biomass was dominated by the picophytoplankton size class, with *Prochlorococcus* and prymnesiophytes the major taxa throughout the EZ but a more diverse assemblage in the DCM.
- Integrated NPP for the EZ ranged from 292 to 352 mg C m^{-2} d^{-1} (Yingling *et al.*, 2022). Nitrate uptake showed a strong daytime maximum, while ammonium uptake exhibited no diel variability. The portion of production supported by NO_3^- uptake was low (1–14%) for the upper EZ and 3–44% in the lower EZ.
- *Prochlorococcus* was a major contributor (113–204 mg C m^{-2} d^{-1}) to productivity, but prymnesiophytes (34–134 mg C m^{-2} d^{-1}) co-dominated in 2017 (Landry *et al.*, 2022). Diatom and dinoflagellate contributions to production were consistently low (generally <10 mg C m^{-2} d^{-1}). Microzooplankton grazing accounted for a mean overall rate of loss of 68 ± 6% of phytoplankton carbon growth but fell far short of balancing the growth rates of bacterial populations.
- Euphotic-zone biomass of mesozooplankton ranged from 101 to 513 mg C m^{-2} during the day and 216 to 798 mg C m^{-2} at night (Landry and Swalethorp, 2022). Grazing on phytoplankton was low (1–3% of Chl*a* consumed d^{-1}), but estimated trophic fluxes from microzooplankton consumption and carnivory were sufficient to satisfy the C demand for respiration and growth of suspension-feeding mesozooplankton estimated from empirical relationships.
- A NEMURO-based (Kishi *et al.*, 2007) physical-biogeochemical model parameterized with BLOOFINZ-GoM rate and relationship data captured broad ecosystem attributes including phytoplankton and mesozooplankton biomass, depth of the DCM and nutricline, and growth and grazing patterns (Shropshire *et al.*, 2020). Regional mesozooplankton production estimated from the model average 66 ± 8 × 10^9 kg C y^{-1}.

- Carbon export efficiency (export/NPP) measured by sediment traps at the EZ base varied from 11 to 25% (Stukel *et al.*, 2022a). Nitrogen export from the EZ base averaged 520 μmol N m^{-2} d^{-1} (range: 462–1 144 μmol N m^{-2} d^{-1}). Changes in pigments, elemental fluxes and isotopic composition of sinking particles indicate substantial particle transformation during transit from the upper EZ into the mesopelagic.
- A nitrogen isotope budget comparing the $\delta^{15}N$ of nitrate with that of sinking particulate N demonstrated that export production is mostly (>80%) supported by subsurface nitrate, with an inconsequential role of N_2 fixation (Knapp *et al.*, 2022). The low $\delta^{15}N$ nitrogen that supports primary production primarily derives from recycled ammonium.
- Stratification strength assessed by Thorpe-scale analyses of vertical eddy diffusivity prevents adequate delivery of nitrate into the EZ to balance N export. Estimates of net lateral transport of organic matter from the outer GoM shelf to the oceanic region, derived independently from satellite-derived remote sensing products and the NEMURO-GoM model, resolve this export balance (Kelly *et al.*, 2021). Lateral transport of zooplankton production from the outer shelf to open ocean is also needed to satisfy the estimated carbon demands of offshore carnivorous zooplankton (Landry and Swalethorp, 2022).

Habitat quality for larval bluefin tuna

Four BLOOFINZ studies evaluate the feeding and growth of ABT larvae within the broader context of food web fluxes in the oceanic GoM. Shiroza *et al.* (2022) investigate the zooplankton prey and ontogenetic feeding selectivity of larvae relative to the availability of prey taxa and sizes during the Lagrangian studies. Malca *et al.* (2022) determine age-length relationships and daily somatic growth estimates based on otolith analysis of the same specimens. Stukel *et al.*, 2022b assimilate process data from the Lagrangian field experiments into a linear inverse ecosystem model to generate mass-balance constrained food-web fluxes for the study region that highlight the flows to ABT larvae. Shropshire *et al.* (2022) evaluate the tradeoffs between larval starvation and predation mortality using an individual-based model that simulates larval dispersal, growth and mortality within spatiotemporally varying predator and prey fields. Significant findings from these studies include the following:

- Dietary composition shifts from smaller (copepod nauplii, appendicularians and ciliates) to larger prey (calanoid copepodids and especially cladocerans)

during larval development (Shiroza *et al.*, 2022). Quantitative importance of ciliates (up to 9% of ingested C) was documented for the first time, and postflexion larvae were shown to be highly selective for cladocerans (up to 70% of ingested C). Diet and prey selection was broader (generalist feeding) when preferred taxa (notably cladocerans) were rare, but narrowed sharply, consistent with active prey selection, when preferred prey were more abundant in C5.

- Growth rates of ABT larvae were similar, on average, 0.37 and 0.39 mm d^{-1} in the C1 (2017) and C5 (2018) habitats, respectively, but they differed significantly through ontogeny (Malca *et al.*, 2022). Otolith growth variability correlated with a food limitation index (Shropshire *et al.*, 2022) based on modeled metabolic requirements relative to ingestion estimates from larval sensory radius and prey biomass concentration. Additionally, growth correlated with ingested prey only when considering prey types preferred across all larval flexion stages (copepod nauplii, cladocerans) and indicated significant growth enhancement in the C5 experiment for larger postflexion larvae feeding extensively on cladocerans. Thus, ontogenetic differences in preferred prey lead to ontogenetic differences in larval growth rates among habitats that differ in both quantity and composition of food resources.
- Despite the microbial loop's dominant role in the oceanic GoM, implying a long inefficient food chain, preferred feeding on prey associated with herbivorous and multivorous trophic pathways allows ABT larvae to achieve relatively low trophic positions (∼4.0 preflexion; ∼4.2 postflexion) that enhance food-web transfer (Stukel *et al.* (2022b).
- Individual-based model results show a shifting trade-off between starvation and predation risks during larval development in the oligotrophic GoM (Shropshire *et al.*, 2022). Spawning areas along the shelf break are found to optimize the tradeoffs when associated with transport of productivity from the large shelf to the offshore region. Shelf proximity provides a nutritional supplement to early larvae for whom starvation is the largest mortality factor, and older larvae benefit from higher survival in the oceanic GoM with fewer predators.

Comparisons to other open-ocean systems

While the BLOOFINZ cruises were not specifically designed to compare GoM characteristics to other open-ocean ecosystems, some useful comparisons were made in areas in which study methods were similar. Based

on FCM-analyzed picophytoplankton populations and HPLC pigment analyses, for example, Selph *et al.* (2022) show similarities and differences in GoM phytoplankton community composition to long-term averages of the Hawaii Ocean Timeseries (HOT) and the Bermuda Atlantic Timeseries Study (BATS). Landry *et al.* (2022) contrast taxon-resolved contributions to phytoplankton production and microzooplankton grazing in the GoM to similar studies in the equatorial Pacific, Costa Rica Dome and subtropical Pacific. Landry and Swalethorp (2022) further compare GoM estimates of mesozooplankton biomass and grazing to seven regions in the tropical and subtropical Pacific, Atlantic and Indian Oceans, including HOT and BATS. Finally, HOT and BATS are among the 19 ocean regions that Stukel *et al.* (2022a) compared with measured export rates and efficiencies in the GoM. Significant conclusions from these comparisons are as follows:

- Mixed-layer (upper 30 m) concentrations of TChl*a* ($40 \pm 11 \, \mu g \, m^{-3}$) in the oceanic GoM in May are less than half the annual mean concentrations at either HOT or BATS, but DCM concentrations are similar ($270–310 \, \mu g \, m^{-3}$) at all three sites (Selph *et al.*, 2022). Concentrations, integrated totals and cell ratios for photosynthetic bacteria fall into the observed ranges at BATS but are less than at HOT for *Prochlorococcus* and greater than at HOT for *Synechococcus*. Major accessory pigments in the GoM suggest lower ML concentrations of all eukaryotic phytoplankton than at HOT or BATS, except for similar concentrations of peridinin-containing dinoflagellates and more prasinophytes compared with HOT. DCM pigments show stronger similarities to HOT for diatoms and prymnesiophytes and to BATS for dinoflagellates and prasinophytes.
- Previous studies showed region-specific characteristics with respect to the relative contributions of phytoplankton groups to production and microzooplankton grazing. The oceanic GoM is similar to the subtropical North Pacific in terms of a dominant role (≥50%) of *Prochlorococcus* and falls intermediate between the equatorial Pacific and Costa Rica Dome in the relative contribution (7–16%) of *Synechococcus*. The GoM is further distinguished by relatively high contributions from prymnesiophytes (14 to ≥40%) and low contributions from diatoms and dinoflagellates (Landry *et al.*, 2022).
- Mesozooplankton biomass in the oceanic GoM is similar to the long-term average for the subtropical Pacific at HOT Stn. ALOHA but higher than measured at BATS or in the subtropical Indian Ocean. However, the ratio of zooplankton carbon

standing stock to mean daily carbon primary production (1.08 in the GoM) is substantially higher than either HOT (0.68) or BATS (0.48) (Landry and Swalethorp, 2022).

• Despite lower primary production, export rates at the base of the EZ are slightly higher than measured for HOT and BATS, leading to higher export ratios of 10–20% in the GoM. Similar to BATS and HOT, subsurface nitrate fuels the majority of export in the GoM (Knapp *et al.*, 2022). Transfer efficiencies through mesopelagic depths are similar in the three regions giving a slightly higher proportion of NPP sequestered in the deep ocean of the GoM (Stukel *et al.*, 2022a).

SUMMARY

BLOOFINZ-GoM cruises combined traditional fisheries approaches within the broader framework of a pelagic biogeochemical and food-web study in order to better understand larval habitat characteristics in one of the major spawning regions of ABT. One insight provided by the lower level process measurements was the lack of a clear productivity benefit to the previously observed association of larvae with the outer edges of loop eddies. Primary production rates were similar in experimental locations with and without ABT larvae (Yingling *et al.*, 2022) and also substantially lower in the larval ABT eddy habitat than long-term averages for subtropical gyres of the Atlantic and Pacific Oceans. *Trichodesmium* spp. abundances were low, consistent with ^{15}N isotope mass balances which revealed an insignificant contribution of N$_2$ fixation to NP and N cycling. The production system of this oligotrophic habitat thus runs mainly on recycled ammonium, with microbial nitrification within the EZ suggested to generate much of the nitrate utilized by phytoplankton.

To contrast with microbial dominance and the relatively low rates of *in situ* productivity in the larval ABT habitat, various lines of evidence point to lateral transport of organic matter from the continental margins to the offshore regions as providing a significant subsidy to the larval ABT habitat. Measured N export in the oceanic region greatly exceeded estimates of new nitrate delivery to the EZ but were consistent with ecosystem model and satellite-based determinations of organic N transport from the shelf margin by currents and mesoscale features (Kelly *et al.*, 2021). The ratio of zooplankton biomass to phytoplankton primary production in the oceanic GoM was 50–100% higher than in trophically balanced ecosystems of the oligotrophic major oceans, implying an advective supplement to offshore waters

(Landry and Swalethorp, 2022). Satisfying the calculated C demands of oceanic carnivorous planktonic taxa also required prey consumption exceeding *in situ* estimates of zooplankton production (Landry and Swalethorp, 2022). These inferences are supported by particle backtracking analyses that clearly illustrate the transport pathways from our study sites with ABT larvae (C1 and C5; Fig. 5) to their origins in higher production areas on the northeastern continental margin, an area of coastal influence that could reasonably also be a source of cladocerans, the preferred prey of ABT larvae (Shiroza *et al.*, 2022), which are associated with higher larval growth rates (Malca *et al.*, 2022). A Lagrangian individual-based foraging model further emphasizes that ABT spawning along the shelf break with subsequent offshore transport provides advantageous growth conditions which simultaneously minimizes the risks of starvation for early larvae and predation for late larvae (Shropshire *et al.*, 2022). Taken together, our results advance the hypothesis that ABT larvae benefit from association with loop eddies not as mechanisms of productivity enrichment per se, but as circulation features that entrain and transport productivity from the shelf break to the offshore oligotrophic region. Waters along the NE continental margin are one area where spawning ABT adults might reliably find conditions that put larvae in favorable circumstances for successful feeding, growth and survival.

The above conclusions have important implications for advancing understanding of distributional relationships and potential climate impacts on ABT larvae in the GoM. They suggest, for example, that previously described probability relationships between mesoscale features and ABT larvae could be refined by considering the differences among eddies in their interactions with the GoM shelf margins. Explicit hypotheses about distributional relationships can also be tested directly in surveys that compare features with known (*a priori*) histories tracked by satellite remote sensing and circulation models. Similarly, understanding interannual variability or projecting future climate change impacts on recruitment success of ABT in the GoM likely depends less on factors that affect general productivity of the offshore region and more on the timing and magnitude of physical circulation effects in specific areas, such as the NE continental margin. To improve models that can relate variability in physical drivers to their ecological effects, additional process studies are needed in areas that the BLOOFINZ experiments did not measure directly but found to be important in enhancing the efficiency of food web coupling to larvae, such as the role of mixotrophs and trophic dynamics of the highly selected prey categories. With improved skill in predicting

the specific conditions (locations) of ABT spawning, it would also be desirable to design future Lagrangian process experiments that quantify survival along with feeding and growth throughout larval development, as opposed to short-term studies, so that differences in initial environmental conditions can be better evaluated and compared in terms of their outcomes.

DATA ARCHIVING

BLOOFINZ-GoM data are available via the National Oceanic and Atmospheric Administration's (NOAA) National Centers for Environmental Information (NCEI) data repository and at BCO-DMO (Biological and Chemical Oceanography Data Management Office) site https://www.bco-dmo.org/program/819631.

SUPPLEMENTARY DATA

Supplementary data is available at *Journal of Plankton Research* online.

ACKNOWLEDGEMENTS

FUNDING

REFERENCES

Alemany, F., Quintanilla, L., Vélez-Belchí, P., García, A., Cortés, D., Rodríguez, J. M., DE Puelles, M. F., González-Pola, C. *et al.* (2010) Characterization of the spawning habitat of Atlantic bluefin tuna and related species in the Balearic Sea (western Mediterranean). *Prog. Oceanogr.*, **86**, 21–38. https://doi.org/10.1016/j.pocean.2010.04.014.

Bakun, A. (2006) Fronts and eddies as key structures in the habitat of marine fish larvae: opportunity, adaptive response and competitive advantage. *Sci. Mar.*, **70**, 105–122. https://doi.org/10.3989/scimar.2006.70s2105.

Bakun, A. (2013) Ocean eddies, predator pits and bluefin tuna: implications of an inferred "low risk-limited payoff" reproductive scheme of a (former) archetypical top predator. *Fish Fish.*, **14**, 424–438. https://doi.org/10.1111/faf.12002.

Bakun, A. and Broad, K. (2003) Environmental 'loopholes' and fish population dynamics: comparative pattern recognition with focus on El Niño effects in the Pacific. *Fish. Oceanogr.*, **12**, 458–473. https://doi.org/10.1046/j.1365-2419.2003.00258.x.

Behrenfeld, M. J., O'Malley, R. T., Siegel, D. A., McClain, C. R., Sarmiento, J. L., Feldman, G. C., Milligan, A. J., Falkowski, P. G. *et al.* (2006) Climate-driven trends in contemporary ocean productivity. *Nature*, **444**, 752–755. https://doi.org/10.1038/nature05317.

Biggs, D. C. (1992) Nutrients, plankton, and productivity in a warm-core ring in the western Gulf of Mexico. *J. Geophys. Res., Oceans*, **97**, 2143–2154. https://doi.org/10.1029/90JC02020.

Biggs, D. C. and Müller-Karger, F. E. (1994) Ship and satellite observations of chlorophyll stocks in interacting cyclone-anticyclone eddy pairs in the western Gulf of Mexico. *J. Geophys. Res., Oceans*, **99**, 7371–7384. https://doi.org/10.1029/93JC02153.

Biggs, D. C. and Ressler, P. H. (2001) Distribution and abundance of phytoplankton, zooplankton, ichthyoplankton, and micronekton in the Deepwater Gulf of Mexico. *Gulf Mex. Sci.*, **19**, 7–29. https://doi.org/10.18785/goms.1901.02.

Block, B. A., Dewar, H., Blackwell, S. B., Williams, T. D., Prince, E. D., Farwell, C. J., Boustany, A., Teo, S. L. H. *et al.* (2001) Migratory movements, depth preferences, and thermal biology of Atlantic bluefin tuna. *Science*, **293**, 1310–1314. https://doi.org/10.1126/science.1061197.

Block, B. A., Teo, S. L. H., Walli, A., Boustany, A., Stokesbury, M. J. W., Farwell, C. J., Weng, K. C., Dewar, H. *et al.* (2005) Electronic tagging and population structure of Atlantic bluefin tuna. *Nature*, **434**, 1121–1127. https://doi.org/10.1038/nature03463.

Bopp, L., Monfray, P., Aumont, O., Dufresne, J. -L., Le Treut, H., Madec, G., Terray, L., Orr, J. C. *et al.* (2001) Potential impact of climate change on marine export production. *Glob. Biogeochem. Cycles*, **15**, 81–99. https://doi.org/10.1029/1999GB001256.

Boustany, A. M., Reeb, C. A. and Block, B. A. (2008) Mitochondrial DNA and electronic tracking reveal population structure of Atlantic bluefin tuna (*Thunnus thynnus*). *Mar. Biol.*, **156**, 13–24. https://doi.org/10.1007/s00227-008-1058-0.

Bracco, A., Choi, J., Joshi, K., Luo, H. and McWilliams, J. C. (2016) Submesoscale currents in the northern Gulf of Mexico: deep phenomena and dispersion over the continental slope. *Ocean Model*, **101**, 43–58. https://doi.org/10.1016/j.ocemod.2016.03.002.

Brannigan, L. (2016) Intense submesoscale upwelling in anticyclonic eddies. *Geophys. Res. Lett.*, **43**, 3360–3369. https://doi.org/10.1002/2016GL067926.

Carlsson, J., McDowell, J. R., Carlsson, J. E. and Graves, J. E. (2007) Genetic identity of YOY bluefin tuna from the eastern and western Atlantic spawning areas. *J. Hered.*, **98**, 23–28. https://doi.org/10.1093/jhered/esl046.

Carlsson, J., McDowell, J. R., Díaz-Jaimes, P., Carlsson, J. E. L., Boles, S. B., Gold, J. R. and Graves, J. E. (2004) Microsatellite and mitochondrial DNA analyses of Atlantic bluefin tuna (*Thunnus thynnus thynnus*) population structure in the Mediterranean Sea. *Mol. Ecol.*, **13**, 3345–3356. https://doi.org/10.1111/j.1365-294X.2004.02336.x.

Chakraborty, S. and Lohrenz, S. E. (2015) Phytoplankton community structure in the river-influenced continental margin of the northern Gulf of Mexico. *Mar. Ecol. Prog. Ser.*, **521**, 31–47. https://doi.org/10.3354/meps11107.

Chérubin, L. M., Morel, Y. and Chassignet, E. P. (2006) Loop current ring shedding: the formation of cyclones and the effect of topography. *J. Phys. Oceanogr.*, **36**, 569–591. https://doi.org/10.1175/JPO2871.1.

Chust, G., Allen, J., Bopp, L., Schrum, C., Holt, J., Tsiaras, K., Zavatarelli, M., Chifflet, M. *et al.* (2014) Biomass changes and trophic amplification of plankton in a warmer ocean. *Glob. Chang. Biol.*, **20**, 2124–2139. https://doi.org/10.1111/gcb.12562.

Davis, T. L. O., Jenkins, G. P. and Young, J. W. (1990) Diel patterns of vertical distribution in larvae of southern bluefin *Thunnus maccoyii*, and other tuna in the East Indian Ocean. *Mar. Ecol. Prog. Ser.*, **59**, 63–74. https://doi.org/10.3354/meps059063.

Domingues, R., Goni, G., Bringas, F., Muhling, B., Lindo-Atichati, D. and Walter, J. (2016) Variability of preferred environmental conditions for Atlantic bluefin tuna (*Thunnus thynnus*) larvae in the Gulf of Mexico during 1993-2011. *Fish. Oceanogr.*, **25**, 320–336. https://doi.org/10.1111/fog.12152.

Doney, S. C., Ruckelshaus, M., Duffy, J. E., Barry, J. P., Chan, F., English, C. A., Galindo, H. M., Galindo, H. M. *et al.* (2012) Climate change impacts on marine ecosystems. *Annu. Rev. Mar. Sci.*, **4**, 11–37. https://doi.org/10.1146/annurev-marine-041911-111611.

Dorado, S., Rooker, J. R., Wissel, B. and Quigg, A. (2012) Isotope baseline shifts in pelagic food webs of the Gulf of Mexico. *Mar. Ecol. Prog. Ser.*, **464**, 37–49. https://doi.org/10.3354/meps09854.

Elliott, B. A. (1982) Anticyclonic rings in the Gulf of Mexico. *J. Phys. Oceanogr.*, **12**, 1292–1309. https://doi.org/10.1175/1520-0485(1982)012<1292:ARITGO>2.0.CO;2.

Fahnenstiel, G., McCormick, M. J., Lang, G. A., Redalje, D. G., Lohrenz, S. E., Markowitz, M., Wagoner, B. and Carrick, H. J. (1995) Taxon-specific growth and loss rates for dominant phytoplankton populations from the northern Gulf of Mexico. *Mar. Ecol. Prog. Ser.*, **117**, 229–239. https://doi.org/10.3354/meps117229.

Fu, W., Randerson, J. T. and Moore, J. K. (2016) Climate change impacts on net primary production (NPP) and export production (EP) regulated by increasing stratification and phytoplankton community structure in the CMIP5 models. *Biogeosciences*, **13**, 5151–5170. https://doi.org/10.5194/bg-13-5151-2016.

García, A., Alemany, F., DE LA Serna, J. M., Oray, I., Karakulak, S., Rollandi, L., Arigò, A. and Mazzola, S. (2004) Preliminary results of the 2004 bluefin tuna larval surveys off different Mediterranean sites (Balearic archipelago, Levantine Sea and the Sicilian Channel). *Col.. Vol. Sci. Pap. ICCAT*, **58**, 1420–1428.

Garcia, A., Alemany, F., Velez-Belchi, P., López-Jurado, J. L., Cortéz, D., DE LA Serna, J. M., González-Pola, C., Rodriguez, J. M. *et al.* (2005) Characterization of the bluefin tuna spawning habitat off the Balearic archipelago in relation to key hydrographic features and associated environmental conditions. *Col. Vol. Sci. Pap. ICCAT*, **58**, 535–549.

Goldstein, J., Heppell, S., Cooper, A., Brault, S. and Lutcavage, M. (2007) Reproductive status and body condition of Atlantic bluefin tuna in the Gulf of Maine, 2000–2002. *Mar. Biol.*, **151**, 2063–2075. https://doi.org/10.1007/s00227-007-0638-8.

Gomez, F. A., Lee, S.-K., Liu, Y., Hernandez, F. J. Jr., Muller-Karger, F. E. and Lamkin, J. T. (2018) Seasonal patterns in phytoplankton biomass across the northern and deep Gulf of Mexico: a numerical model study. *Biogeosciences*, **15**, 3561–3576. https://doi.org/10.5194/bg-15-3561-2018.

Habtes, S., Muller-Karger, F. E., Roffer, M. A., Lamkin, J. T. and Muhling, B. A. (2014) A comparison of sampling methods for larvae of medium and large epipelagic fish species during spring SEAMAP ichthyoplankton surveys in the Gulf of Mexico. *Limnol. Oceanogr. Meth.*, **12**, 86–101. https://doi.org/10.4319/lom.2014.12.86.

Hidalgo-González, R. M. and Alvarez-Borrego, S. (2008) Water column structure and phytoplankton biomass profiles in the Gulf of Mexico. *Cienc. Mar.*, **34**, 197–212. https://doi.org/10.7773/cm.v34i2.1371.

Hidalgo-González, R. M., Alvarez-Borrego, S., Fuentes-Yaco, C. and Platt, T. (2005) Satellite-derived total and new phytoplankton production in the Gulf of Mexico. *Indian J. Mar. Sci.*, **34**, 408–417.

Hjort, J. (1914) Fluctuations in the great fisheries of northern Europe viewed in the light of biological research. *Rapp. P.-V. Réun. Cons. Int. Explor. Mer*, **20**, 1–228.

Holl, C. M., Villareal, T. A., Payne, C. D., Clayton, T. D., Hart, C. and Montoya, J. P. (2007) *Trichodesmium* in the western Gulf of Mexico: $^{15}N_2$-fixation and natural abundance stable isotope evidence. *Limnol. Oceanogr.*, **52**, 2249–2259. https://doi.org/10.4319/lo.2007.52.5.2249.

Houde, E. D. (1987) Fish early life dynamics and recruitment variability. *Amer. Fish. Soc. Symp. Ser.*, **2**, 17–29.

Hung, C.-C., Guo, L., Roberts, K. A. and Santschi, P. H. (2004) Upper Ocean carbon flux determined by the ^{234}Th approach and sediment traps using size-fractionated POC and ^{234}Th data from the Gulf of Mexico. *Geochem. J.*, **38**, 601–611. https://doi.org/10.2343/geochemj.38.601.

Hung, C.-C., Xu, C., Santschi, P. H., Zhang, S.-J., Schwehr, K. A., Quigg, A., Guo, L., Gong, G.-C. *et al.* (2010) Comparative evaluation of sediment trap and ^{234}Th-derived POC fluxes from the upper oligotrophic waters of the Gulf of Mexico and the subtropical northwestern Pacific Ocean. *Mar. Chem.*, **121**, 132–144. https://doi.org/10.1016/j.marchem.2010.03.011.

Johnstone, C., Pérez, M., Malca, E., Quintanilla, J. M., Gerard, T., Lozano-Peral, D., Alemany, F., Lamkin, J. *et al.* (2021) Genetic connectivity between Atlantic bluefin tuna larvae spawned in the Gulf of Mexico and in the Mediterranean Sea. *PeerJ*, **9**, e11568. https://doi.org/10.7717/peerj.11568.

Kelly, T. B., Knapp, A. N., Landry, M. R., Selph, K. E., Shropshire, T. A., Thomas, R. and Stukel, M. R. (2021) Lateral advection supports nitrogen export in the oligotrophic open-ocean Gulf of Mexico. *Nat. Commun.*, **12**, 3325. https://doi.org/10.1038/s41467-021-23678-9.

Kishi, M. J., Kashiwai, M., Ware, D. M., Megrey, B. A., Eslinger, D. L., Werner, F. E., Noguchi-Aita, M., Azumaya, T. *et al.* (2007) NEMURO - a lower trophic level model for the North Pacific marine ecosystem. *Ecol. Model.*, **202**, 12–25. https://doi.org/10.1016/j.ecolmodel.2006.08.021.

Knapp, A. N., Thomas, R., Stukel, M. R., Kelly, T. B., Landry, M. R., Selph, K. E., Malca, E., Gerard, T. *et al.* (2022) Constraining the sources of nitrogen fueling export production in the Gulf of Mexico using nitrogen isotope budgets. *J. Plankton Res.*, fbab049. https://doi.org/10.1093/plankt/fbab049.

Laiz-Carrión, R., Gerard, T., Suca, J. J., Malca, E., Uriarte, A., Quintanilla, J. M., Privoznik, S., Llopiz, J. K. *et al.* (2019) Stable isotope analysis indicates resource partitioning and trophic niche overlap in larvae of four tuna species in the Gulf of Mexico. *Mar. Ecol. Prog. Ser.*, **619**, 53–68. https://doi.org/10.3354/meps12958.

Laiz-Carrión, R., Gerard, T., Uriarte, A., Malca, E., Quintanilla, J. M., Muhling, B. A., Alemany, F., Privoznik, S. *et al.* (2015)

Trophic ecology of Atlantic Bluefin tuna (Thunnusthynnus) larvae from the Gulf of Mexico and NW Mediterranean spawning grounds: a comparative stable isotope study. *PLoS One*, **10**, e0133406. https://doi.org/10.1371/journal.pone.0133406.

Landry, M. R., Beckley, L. E. and Muhling, B. A. (2019) Climate sensitivities and uncertainties in food-web pathways supporting larval bluefin tuna in subtropical oligotrophic oceans. *ICES J. Mar. Sci.*, **76**, 359–369. https://doi.org/10.1093/icesjms/fsy184.

Landry, M. R., Ohman, M. D., Goericke, R., Stukel, M. R. and Tsyrkevich, K. (2009) Lagrangian studies of phytoplankton growth and grazing relationships in a coastal upwelling ecosystem off Southern California. *Prog. Oceanogr.*, **83**, 208–216. https://doi.org/10.1016/j.pocean.2009.07.026.

Landry, M. R., Selph, K. E., Stukel, M. R., Swalethorp, R., Kelly, T. B., Beatty, J. L. and Quackenbush, C. R. (2022) Microbial food web dynamics in the oceanic Gulf of Mexico. *J. Plankton Res.*, fbab021. https://doi.org/10.1093/plankt/fbab021.

Landry, M. R. and Swalethorp, R. (2022) Mesozooplankton biomass, grazing and trophic structure in the bluefin tuna spawning area of the oceanic Gulf of Mexico. *J. Plankton Res.*, fbab008. https://doi.org/10.1093/plankt/fbab008.

Leipper, D. F. (1970) A sequence of current patterns in the Gulf of Mexico. *J. Geophys. Res.*, **75**, 637–657. https://doi.org/10.1029/JC075i003p00637.

Lindo-Atichati, D., Bringas, F., Goni, G., Muhling, B., Muller-Karger, F. E. and Habtes, S. (2012) Varying mesoscale structures influence larval fish distribution in the northern Gulf of Mexico. *Mar. Ecol. Prog. Ser.*, **463**, 245–257. https://doi.org/10.3354/meps09860.

Liu, H. and Dagg, M. (2003) Interactions between nutrients, phytoplankton growth, and micro- and mesozooplankton grazing in the plume of the Mississippi River. *Mar. Ecol. Prog. Ser.*, **258**, 31–42. https://doi.org/10.3354/meps258031.

Llopiz, J. K., Cowen, R. K., Hauff, M. J., Ji, R., Munday, P. L., Muhling, B. A., Peck, M. A., Richardson, D. E. *et al.* (2014) Early life history and fisheries oceanography: new questions in a changing world. *Oceanography*, **27**, 26–41. https://doi.org/10.5670/oceanog.2014.84.

Llopiz, J. K., Muhling, B. A. and Lamkin, J. T. (2015) Feeding dynamics of Atlantic bluefin tuna (*Thunnus thynnus*) larvae in the Gulf of Mexico. *Coll. Sci. Pap., ICCATT*, **71**, 1710–1715.

Lohrenz, S. E., Fahnenstiel, G. L., Redalje, D. G., Lang, G. A., Dagg, M. J., Whitledge, T. E. and Dortch, Q. (1999) Nutrients, irradiance, and mixing as factors regulating primary production in coastal waters impacted by the Mississippi River plume. *Cont. Shelf Res.*, **19**, 1113–1141. https://doi.org/10.1016/S0278-4343(99)00012-6.

Lohrenz, S. E., Redalje, D. G., Cai, W. J., Acker, J. and Dagg, M. (2008) A retrospective analysis of nutrients and phytoplankton productivity in the Mississippi River plume. *Cont. Shelf Res.*, **28**, 1466–1475. https://doi.org/10.1016/j.csr.2007.06.019.

Lutcavage, M. E., Brill, R. W., Skomal, G. B., Chase, B. C. and Howey, P. W. (1999) Results of pop-up satellite tagging of spawning size class fish in the Gulf of Maine: do North Atlantic bluefin tuna spawn in the mid-Atlantic? *Can. J. Fish. Aquat. Sci.*, **56**, 173–177. https://doi.org/10.1139/f99-016.

Malca, E., Muhling, B., Franks, J., García, A., Tilley, J., Gerard, T., Ingram, W. Jr. and Lamkin, J. T. (2017) The first larval age and growth curve for bluefin tuna (*Thunnus thynnus*) from the Gulf of Mexico: comparisons to the straits of Florida, and the Balearic Sea (Mediterranean). *Fish. Res.*, **190**, 24–33. https://doi.org/10.1016/j.fishres.2017.01.019.

Malca, E., Shropshire, T., Landry, M. R., Quintanilla, J. M., Laiz-Carrion, R., Shiroza, A., Stukel, M. R., Lamkin, J. *et al.* (2022) Influence of food quality on larval growth of Atlantic bluefin tuna (*Thunnus thynnus*) in the Gulf of Mexico. *J. Plankton Res.*, fbac024. https://doi.org/10.1093/plankt/fbac024.

Maul, G. A. and Vukovich, F. M. (1993) The relationship between variations in the Gulf of Mexico loop current and straits of Florida volume transport. *J. Phys. Oceanogr.*, **23**, 785–796. https://doi.org/10.1175/1520-0485(1993)023<0785:TRBVIT>2.0.CO;2.

Melo Gonzalez, N., Muller-Karger, F. E., Cerdeira Estrada, R. S., Perez, R., Victoria, I., Cardennas Perez, P. and Arenal, I. M. (2000) Near-surface phytoplankton distribution in the western intra-Americas sea: the influence of El Nino and weather events. *J. Geophys. Res., Oceans*, **105**, 14029–14043. https://doi.org/10.1029/2000JC900017.

Merino, M. (1997) Upwelling on the Yucatan shelf: hydrographic evidence. *J. Mar. Syst.*, **13**, 101–121. https://doi.org/10.1016/S0924-7963(96)00123-6.

Mitra, A., Castellani, C., Gentleman, W. C., Jónasdóttir, S. H., Flynn, K. J., Bode, A., Halsband, C., Kuhn, P. *et al.* (2014) Bridging the gap between marine biogeochemical and fisheries sciences; configuring the zooplankton link. *Prog. Oceanogr.*, **129**, 176–199. https://doi.org/10.1016/j.pocean.2014.04.025.

Muhling, B. A., Brodie, S., Smith, J. A., Tommasi, D., Gaitan, C. F., Hazen, E. L., Jacox, M. G., Auth, T. D. *et al.* (2020) Predictability of species distributions deteriorates under novel environmental conditions in the California current system. *Front. Mar. Sci.*, **7**, 589. https://doi.org/10.3389/fmars.2020.00589.

Muhling, B. A., Lamkin, J. T., Alemany, F., García, A., Farley, J. H., Ingram, G. W. Jr., Berastegui, D. A., Reglero, P. *et al.* (2017) Reproduction and larval biology in tunas, and the importance of restricted area spawning grounds. *Rev. Fish Biol. Fish.*, **27**, 697–732. https://doi.org/10.1007/s11160-017-9471-4.

Muhling, B. A., Lee, S.-K., Lamkin, J. T. and Liu, Y. (2011) Predicting the effects of climate change on bluefin tuna (*Thunnus thynnus*) spawning habitat in the Gulf of Mexico. *ICES J. Mar. Sci.*, **68**, 1051–1062. https://doi.org/10.1093/icesjms/fsr008.

Muhling, B. A., Lamkin, J. T. and Roffer, J. T. (2010) Predicting the occurrence of Atlantic bluefin tuna (*Thunnus thynnus*) larvae in the northern Gulf of Mexico: building a classification model from archival data. *Fish. Oceanogr.*, **19**, 526–539. https://doi.org/10.1111/j.1365-2419.2010.00562.x.

Mulholland, M. R., Bernhardt, P. W., Heil, C. A., Bronk, D. A. and O'Neil, J. M. (2006) Nitrogen fixation and release of fixed nitrogen by *Trichodesmium* spp. in the Gulf of Mexico. *Limnol. Oceanogr.*, **51**, 1762–1776. https://doi.org/10.4319/lo.2006.51.4.1762.

Mulholland, M. R., Bernhardt, P. W., Ozmon, I., Procise, L. A., Garrettb, M., O'Neil, J. M., Heil, C. A. and Bronk, D. A. (2014) Contribution of diazotrophy to nitrogen inputs supporting *Karenia brevis* blooms in the Gulf of Mexico. *Harmful Algae*, **38**, 20–29. https://doi.org/10.1016/j.hal.2014.04.004.

Müller-Karger, F. E., Smith, J. P., Werner, S., Chen, R., Roffer, M., Liu, Y., Muhling, B., Lindo-Atichati, D. *et al.* (2015) Natural variability of surface oceanographic conditions in the offshore Gulf of Mexico. *Prog. Oceanogr.*, **134**, 54–76. https://doi.org/10.1016/j.pocean.2014.12.007.

Nishikawa, Y., Honma, M., Ueyanagi, S. and Kikawa, S. (1985) Average distribution of larvae of oceanic species of scombrid fishes, 1956–1981. *Far Seas Fish. Res. Lab. S. Ser.*, **12**, 1–99.

Olson, E. M., McGillicuddy, D. J. Jr., Flierl, G. R., Davis, C. S., Dyhrman, S. T. and Waterbury, J. B. (2015) Mesoscale eddies and *Trichodesmium* spp. distributions in the southwestern North Atlantic. *J. Geophys. Res., Oceans*, **120**, 4129–4150. https://doi.org/10.1002/2015JC010728.

Puncher, G. N., Cariani, A., Maes, G. E., Van Houdt, J., Herten, K., Cannas, R., Rodriguez-Ezpeleta, N., Albaina, A. *et al.* (2018) Spatial dynamics and mixing of bluefin tuna in the Atlantic Ocean and Mediterranean Sea revealed using next-generation sequencing. *Mol. Ecol. Resour.*, **18**, 620–638. https://doi.org/10.1111/1755-0998.12764.

Qian, Y., Jochens, A. E., Kennicutt, M. C. II and Biggs, D. C. (2003) Spatial and temporal variability of phytoplankton biomass and community structure over the continental margin of the Northeast Gulf of Mexico based on pigment analysis. *Cont. Shelf Res.*, **23**, 1–17. https://doi.org/10.1016/S0278-4343(02)00173-5.

Rabalais, N., Turner, R. E., Dortch, Q, Justic, D., Bierman, V. Jr. and Wiseman, W. Jr. (2002) Nutrient-enhanced productivity in the northern Gulf of Mexico: past, present and future. *Hydrobiologia*, **475/476**, 39–63. https://doi.org/10.1023/A:1020388503274.

Richards, W. J. (1977) A further note on Atlantic bluefin tuna spawning. *Collect. Vol. Sci. Pap. ICCAT*, **6**, 335–336.

Richards, W. J. (2005) Scombridae: mackerels and tunas. In Richards, W. J. (ed.), *Early Stages of Atlantic Fishes: An Identification Guide for the Western Central North Atlantic Ocean*, Vol. **2**, CRC Press, Boca Raton, pp. 2187–2227.

Richardson, D. E., Marancik, K. E., Guyon, J. R., Lutcavage, M. E., Galuardi, B., Lam, C. H., Walsh, H. J., Wildes, S. *et al.* (2016) Discovery of a spawning ground reveals diverse migration strategies in Atlantic bluefin tuna (*Thunnus thynnus*). *Proc. Natl. Acad. Sci. U. S. A.*, **113**, 3299–3304. https://doi.org/10.1073/pnas.1525636113.

Rodríguez-Ezpeleta, N., Díaz-Arce, N., Walter, J. F., Richardson, D. E., Rooker, J. R., Nøttestad, L., Hanke, A. R., Franks, J. S. *et al.* (2019) Determining natal origin for improved management of Atlantic bluefin tuna. *Front. Ecol. Environ.*, **17**, 439–444. https://doi.org/10.1002/fee.2090.

Rodríguez-Marín, E., Barreiro, S., Montero, F. E. and Carbonell, E. (2008) Looking for skin and gill parasites as biological tags for Atlantic bluefin tuna (*Thunnus thynnus*). *Aquat. Living Resour.*, **21**, 365–371. https://doi.org/10.1051/alr:2008054.

Rooker, J. R., Alvarado Bremer, J. R., Block, B. A., Dewar, H., DE Metrio, G., Corriero, A., Krause, R. T., Prince, E. D. *et al.* (2007) Life history and stock structure of Atlantic bluefin tuna (*Thunnus thynnus*). *Rev. Fish. Sci.*, **15**, 265–310. https://doi.org/10.1080/10641260701484135.

Rooker, J. R., Secor, D. H., De Metrio, G., Schloesser, R., Block, B. A. and Neilson, J. D. (2008) Natal homing and connectivity in Atlantic bluefin tuna populations. *Science*, **322**, 742–744. https://doi.org/10.1126/science.1161473.

Rooker, J. R., Secor, D. H., Zdanowicz, V. S., De Metrio, G. and Relini, L. O. (2003) Identification of Atlantic bluefin tuna (*Thunnus thynnus*) stocks from putative nurseries using otolith chemistry. *Fish. Oceanogr.*, **12**, 75–84. https://doi.org/10.1046/j.1365-2419.2003.00223.x.

Rykaczewski, R. R. and Dunne, J. P. (2010) Enhanced nutrient supply to the California current ecosystem with global warming and increased stratification in an earth system model. *Geophys. Res. Lett.*, **37**, L21606. https://doi.org/10.1029/2010GL045019.

Schaefer, K. M. (2001) Reproductive biology. In Block, B. A. and Stevens, E. D. (eds), *Tunas: Physiology, Ecology and Evolution*. Academic Press, San Diego, pp. 225–270, https://doi.org/10.1016/S1546-5098(01)19007-2.

Scott, G. P., Turner, S. C., Churchill, G. B., Richards, W. J. and Brothers, E. B. (1993) Indices of larval bluefin tuna, *Thunnus thynnus*, abundance in the Gulf of Mexico; modelling variability in growth, mortality, and gear selectivity. *Bull. Mar. Sci.*, **53**, 912–929.

Selph, K. E., Swalethorp, R., Stukel, M. R., Kelly, T. B., Knapp, A. N., Fleming, K., Hernandez, T. and Landry, M. R. (2022) Phytoplankton community composition and biomass in the open-ocean Gulf of Mexico. *J. Plankton Res.*, fbab006. https://doi.org/10.1093/plankt/fbab006.

Shimose, T. and Farley, J. H. (2016) Age, growth and reproductive biology of bluefin tunas. In Kitagawa, T. and Kimura, S. (eds.), *Biology and Ecology of Bluefin Tuna*, CRC Press, Boca Raton, FL, pp. 47–77.

Shiroza, A., Malca, E., Lamkin, J. T., Gerard, T., Landry, M. R., Stukel, M. R., Laiz-Carrión, R. and Swalethorp, R. (2022) Active prey selection in developing larvae of Atlantic Bluefin tuna (*Thunnus thynnus*) in spawning grounds of the Gulf of Mexico. *J. Plankton Res.*, fbab020. https://doi.org/10.1093/plankt/fbab020.

Shropshire, T., Morey, S. L., Chassignet, E., Bozec, V. A., Coles, V. J., Landry, M. R., Swalethorp, R., Zapfe, G. *et al.* (2020) Quantifying spatiotemporal variability in zooplankton dynamics in the Gulf of Mexico with a physical-biogeochemical model. *Biogeosciences*, **17**, 3385–3407. https://doi.org/10.5194/bg-17-3385-2020.

Shropshire, T. A., Morey, S. L., Chassignet, E. P., Karnauskas, M., Coles, V. J., Malca, E., Laiz-Carrión, R., Fiksen, Ø. *et al.* (2022) Trade-offs between risks of predation and starvation in larvae make the shelf break an optimal spawning location for Atlantic Bluefin tuna. *J. Plankton Res.*, fbab041. https://doi.org/https://doi.org/10.1093/plankt/fbab041.

Strom, S. L. and Strom, M. W. (1996) Microplankton growth, grazing, and community structure in the northern Gulf of Mexico. *Mar. Ecol. Prog. Ser.*, **130**, 229–240. https://doi.org/10.3354/meps130229.

Stukel, M. R., Benitez-Nelson, C., Décima, M., Taylor, A. G., Buchwald, C. and Landry, M. R. (2016) The biological pump in the Costa Rica dome: an open-ocean upwelling system with high new production and low export. *J. Plankton Res.*, **38**, 348–365. https://doi.org/10.1093/plankt/fbv097.

Stukel, M. R., Girard, T., Kelly, T. B., Knapp, A. N., Laiz-Carrión, R., Lamkin, J. T., Landry, M. R., Malca, E. *et al.* (2022b) Plankton food webs in the oligotrophic Gulf of Mexico spawning grounds of Atlantic Bluefin tuna. *J. Plankton Res.*, fbab023. https://doi.org/10.1093/plankt/fbab023.

Stukel, M. R., Kahru, M., Benitez-Nelson, C. R., Decima, M., Goericke, R., Landry, M. R. and Ohman, M. D. (2015) Using Lagrangian-based process studies to test satellite algorithms of vertical carbon flux in the eastern North Pacific Ocean. *J. Geophys. Res., Oceans*, **120**, 7208–7222. https://doi.org/10.1002/2015JC011264.

Stukel, M. R., Kelly, T. B., Landry, M. R., Selph, K. E. and Swalethorp, R. (2022a) Sinking carbon, nitrogen, and pigment flux within and beneath the euphotic zone in the oligotrophic, open-ocean Gulf of Mexico. *J. Plankton Res.*, fbab001. https://doi.org/10.1093/plankt/fbab001.

Teo, S. L., Boustany, A., Dewar, H., Stokesbury, M. J., Weng, K. C., Beemer, S., Seitz, A. C., Farwell, C. J. *et al.* (2007) Annual migrations, diving behavior, and thermal biology of Atlantic bluefin tuna, *Thunnus thynnus*, on their Gulf of Mexico breeding grounds. *Mar. Biol.*, **151**, 1–18. https://doi.org/10.1007/s00227-006-0447-5.

Tilley, J. D., Butler, C. M., Suárez-Morales, E., Franks, J. S., Hoffmayer, E. R., Gibson, D. P., Comyns, B. H., Ingram, G. W. Jr. *et al.* (2016) Feeding ecology of larval Atlantic bluefin tuna, *Thunnus thynnus*, from the Central Gulf of Mexico. *Bull. Mar. Sci.*, **92**, 321–334. https://doi.org/10.5343/bms.2015.1067.

Vukovich, F. M. (2007) Climatology of ocean features in the Gulf of Mexico using satellite remote sensing data. *J. Phys. Oceanogr.*, **37**, 689–707. https://doi.org/10.1175/JPO2989.1.

Wawrik, B. and Paul, J. H. (2004) Phytoplankton community structure and productivity along the axis of the Mississippi River plume in oligotrophic Gulf of Mexico waters. *Aquat. Microb. Ecol.*, **35**, 185–196. https://doi.org/10.3354/ame035185.

Yingling, N., Kelly, T. B., Shropshire, T. A., Landry, M. R., Selph, K. E., Knapp, A. N., Kranz, S. A. and Stukel, M. R. (2022) Taxon-specific phytoplankton growth, nutrient utilization and light limitation in the oligotrophic Gulf of Mexico. *J. Plankton Res.*, fbab028. https://doi.org/10.1093/plankt/fbab028.

Yoder, J. A., Ackleson, S. G., Barber, R. T., Flament, P. and Balch, W. M. (1994) A line in the sea. *Nature*, **371**, 689–692. https://doi.org/10.1038/371689a0.

Zimmerman, R. A. and Biggs, D. G. (1999) Patterns of distribution of sound-scattering zooplankton in warm- and cold-core eddies in the Gulf of Mexico, from a narrowband acoustic Doppler current profiler survey. *J. Geophys. Res.*, **104**, 5251–5262. https://doi.org/10.1029/1998JC900072.